

Applications of the Lagged Normal Density Curve as a Model for Arterial Dilution Curves

By James B. Bassingthwaite, M.D., Ph.D., Francis H. Ackerman, and Earl H. Wood, M.D., Ph.D.

■ The dispersion of an indicator in a flowing liquid increases with time and with the distance travelled. The form of the dispersion and its rate of increase have only recently come to the attention of investigators. Poiseuille's model, parabolic flow, has been used as an approximate description of flow in the vascular system in spite of the fact that there are a priori reasons for expecting it to be unsuitable. The observations by Griffiths,¹ Hull and Kent,² and G. Taylor^{3,4} were that spatial dispersion of indicator in fluids flowing through rigid tubes was symmetric and nearly Gaussian. Sheppard⁵ had arrived independently at the hypothesis that this might also be true for the vascular system and had begun a series of experiments using the random walk equation as a model.

In the present study on normal men, the lagged normal density curve^{6,7} was used to describe the primary portion of recorded curves. From the resultant concise descriptions of the data, further analyses of flow characteristics and dispersion were made, which led to the inescapable, yet far from new, conclusion that, in the arterial system, the flow profile is not parabolic but is blunter and is probably always somewhat turbulent.

The nomenclature of this study is intended to be in accordance with that standardized by Wood.⁸

The Model

The random dispersion occurring with turbu-

From the Mayo Clinic and Mayo Foundation, Rochester, Minnesota.

Supported in part by Research Grants HE-04664, HE-09719, and FR-00007 from the National Institutes of Health, U. S. Public Health Service.

Accepted for publication October 11, 1965.

lence and pulsatile flow suggests the use of the equation for a normal density curve (fig. 1):

$$h_1(t) = \frac{1}{\sigma(2\pi)^{1/2}} \cdot e^{-1/2[(t-t_c)/\sigma]^2}$$

$$h_1(t) = 0 \quad \begin{array}{l} \text{for } t \geq 0 \text{ and} \\ \text{for } t < 0. \end{array} \quad (1)$$

$h_1(t)$ is a frequency function of unit area, representing a symmetric random distribution of transit times of the indicator about a central time, t_c (seconds), with standard deviation, σ . This is a Gaussian curve; it is often colloquially called a normal distribution curve, but this name refers more properly⁹ to its sigmoid-shaped integral, the cumulative frequency distribution curve.

The occurrence of mixing in cardiac chambers, in the aorta during diastole, and in eddy currents at points of vessel branching, as well as the observation that dye curves are always skewed, suggests that a first-order exponential process may also be involved:

$$h_2(t) = \frac{1}{\tau} \cdot e^{-t/\tau} \text{ for } t \geq 0 \text{ and} \quad (2)$$

$$h_2(t) = 0 \quad \text{for } t < 0.$$

τ is the time constant and $h_2(t)$ has unit area. (Flow through a hypothetical mixing chamber washes out indicator at a rate such that the concentration at the end of an interval of duration, τ , is $1/e$ ($= 1/2.718 = 0.37$) of its initial value).

The convolution of these two equations, representing the sequential or simultaneous effect of one process on the distribution produced by the other may be described by the differential equation:

$$h_3(t) = \frac{1}{\sigma(2\pi)^{1/2}} \cdot e^{-1/2[(t-t_c)/\sigma]^2} - \tau \frac{dh_3(t)}{dt} \quad (3)$$

which also has unit area. The three parameters, σ , τ , and t_c , provide a complete description of the curve's shape and position in time. The mean transit time, \bar{t} , of the model is $t_c + \tau$, the vari-

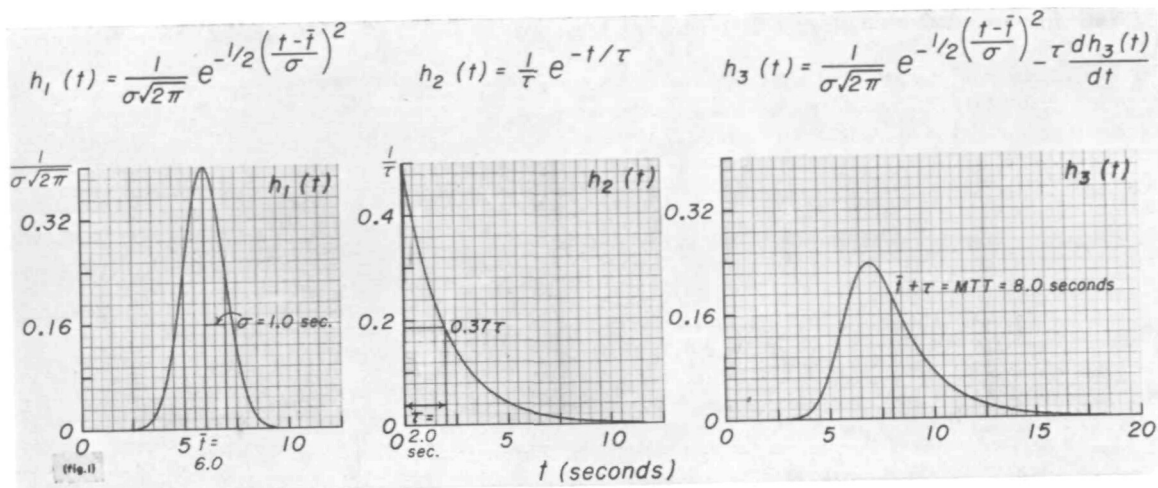


FIGURE 1

Model for indicator dilution curves. Left panel: normal density curve. Middle panel: single exponential. Right panel: lagged normal density curve.

ance is $\sigma^2 + \tau^2$, and the third moment is $2\tau^3$. Equation 3 could be given equally well as the convolution integral:

$$h_3(t) = \int_0^t h_1(\lambda) h_2(t - \lambda) d\lambda \quad (3a)$$

in which λ is the dummy variable of integration and increases from zero to t during the integration. In applying this equation to concentration-time curves in the circulation,

$$C(t) = m_i/Q \cdot h_3(t) \quad (3b)$$

in which m_i (mg) is the amount of indicator injected, Q (liters/sec) is the flow rate, and m_i/Q is the area of the curve. Hereafter, equation 3b is referred to as "the model."

Methods

Five men, 25 to 33 years of age, served as subjects. They were given 100 mg of secobarbital as premedication. During the experiment they rested supine on a padded fluoroscopic table. For two periods of 30 to 50 minutes during each experiment, adenosine triphosphate (ATP), 1.0 mg/ml in Ringer's solution, was infused into the right common iliac artery at a rate of either 0.5 or 1.0 mg/min. This produced marked increases of blood flow in the right leg.

NEEDLE AND CATHETER POSITIONS

The following were introduced by percutaneous needle puncture:

1. A 70-cm Lehman no. 5 catheter, inserted via the right medial antecubital vein, was advanced into the superior vena cava just above the right atrium, for injection of dye.

2. An 80-cm Afford* catheter (internal diameter, 0.5 mm; external diameter, 0.8 mm), introduced into the left femoral artery at the level of the inguinal ligament, was advanced a distance equal to 5 cm less than the distance from the groin to the third intercostal space at the sternal border, for injection of dye into the lower thoracic aorta.

3. A no. 20 thin-walled needle was inserted into the right dorsalis pedis artery on the dorsum of the foot, for sampling.

4. A special assembly for combined dye injection and blood sampling was used at the right femoral artery. A no. 17 thin-walled needle was introduced into the artery and through it a 40-cm thick-walled Afford catheter (internal diameter, 0.25 mm; external diameter, 0.8 mm) was introduced and advanced 8 to 9 cm beyond the needle tip. This assembly was used for injection of dye via the Afford catheter and for continuous sampling of blood through the needle around the catheter via the side arm leading to the densitometer.

5. A no. 19 thin-walled needle was introduced into the right femoral artery and a 40-cm thin-walled Afford catheter (internal diameter, 0.50 mm; external diameter, 0.8 mm) and was advanced 8 to 10 cm beyond the tip of the needle. This was used for the infusion of ATP.

DYE INJECTION

Indocyanine green,†¹⁰ at a concentration of

*A radiopaque polyvinyl catheter made by Mr. A. E. Afford, 340 Marne Avenue, Haddonfield, New Jersey.

†Cardio-Green, Hynson, Westcott and Dunning, Inc., Baltimore, Maryland.

2.5 mg/ml, was used as indicator. For each experiment, 200 mg of the dye were dissolved in 10 ml of water, 4 ml of 20% human serum albumin were added to stabilize the indocyanine green solution, and isotonic Ringer's solution was added to make a final volume of 80 ml. The same solution was used for making up the calibration dilutions for the densitometers.

Dye solution was injected by means of a pneumatically driven syringe¹¹ and the duration of the injection was regulated with an electrically operated solenoid valve. The syringe movement was recorded via a linear potentiometer mechanically in parallel to it. The amount of dye injected, m_i (mg), was calculated from the equation, $m_i = Cd(V/D)$, in which C is concentration of the dye solution (mg/ml), d is deflection (cm) produced by the syringe movement, and D is the deflection (cm) recorded when the syringe was emptied of a known volume, V (ml). The injections were accomplished in 0.6 to 1.0 second; the time at which the syringe was at the midpoint of its movement was used as zero time for the indicator dilution curves.

SAMPLING SYSTEMS

Blood was withdrawn from the femoral and dorsalis pedis arteries with a Harvard constant-rate sampling device* at a constant rate of 9.8 to 10.0 ml/min. The differences in rates were due to differences in diameters of the barrels of the 30-ml glass syringes used; therefore, each rate was checked by timed withdrawal of water from a graduated cylinder.

The dynamic response of each sampling system was determined, with blood, by recording the response to a step change in indicator concentration at the tip of the needle, as described by Fox and co-workers.¹² The volumes of the two systems (at femoral and dorsalis pedis arteries) were adjusted so that their dynamic responses were similar (fig. 2). The femoral system consisted of needle (with Afford catheter filling part of the lumen), right-angled adapter, 10 cm of nylon tubing (internal diameter, 1.0 mm; external diameter, 1.8 mm), three-way stopcock, and densitometer. The stopcocks allowed thorough flushing of the sampling system without introducing large quantities of saline into the subject. The total volumes of the sampling systems from needle tip to densitometer lumen were 0.5 to 0.6 ml and, therefore, caused significant distortion of the indicator dilution curves. However, the magnitude of this distortion was not great and was similar at the two sampling sites. The

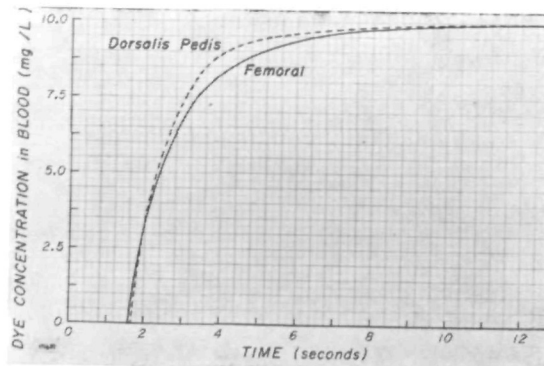


FIGURE 2

Responses of the sampling systems to step changes in dye concentration. During sampling at 10 ml/min, the undyed blood at the tip of the sampling system was suddenly replaced by blood containing indocyanine green (10 mg/liter). The response of the system used at the femoral artery was slower than that at the dorsalis pedis artery. The difference in mean transit times was about 0.3 second.

data presented in this paper are from the uncorrected curves.

DENSITOMETRY

The densitometers* selected have their greatest sensitivity at 800 $m\mu$, the absorption maximum of the dye. The light sensor is a photoconductive cell which forms one limb of a Wheatstone bridge; the output voltage from a properly adjusted instrument is linearly related to dye concentration over the range of 0 to 40 mg/liter.

The dynamic response of the photocell, circuitry, and galvanometer for each densitometer was tested by recording the output when a wire was rapidly withdrawn from the lumen of the densitometer (this produces a step change in incident light intensity). The 90 and 98% response times of both instruments were 0.09 and 0.15 second, respectively.

For calibration of the densitometers (fig. 3), dilutions were made up by the addition of 0.01, 0.02, 0.03, 0.04, and 0.05 ml of a solution of dye (2.5 mg/ml) to 10.0 ml of whole blood. Blood was drawn through the densitometers in tandem at a constant rate of 10 ml/min. The deflection produced by the densitometer was set to a base line when undyed blood was flowing through the lumen (sensitivity potentiometer setting, P_0). With blood containing dye at 2.5 mg/liter flowing through the lumen, the deflection was recorded and the galvanometer beam was reset to the base line by adjusting the sen-

*Harvard Apparatus Company, Dover, Massachusetts.

*XC250A made by Waters Company, Rochester, Minnesota.

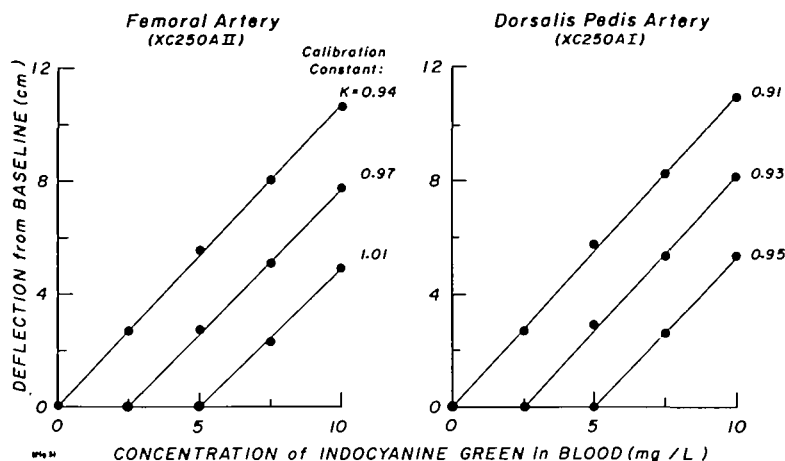


FIGURE 3

Calibration of two densitometers for indocyanine green in whole blood. Calibration was done on blood containing no background dye (lines passing through the origin) and on blood having background dye levels of 2.5 or 5.0 mg/liter (lines intercepting the abscissa at 2.5 and 5.0). The increase in calibration constant (decrease in slope) with higher background dye levels indicates a loss in sensitivity.

sitivity potentiometer (to setting $P_{2.5}$). The potentiometer was then reset to P_0 , blood containing dye at 5.0 mg/liter was drawn through the lumen, the deflection was recorded, the potentiometer was reset to $P_{2.5}$, the deflection was recorded, and then the potentiometer was adjusted to reset the galvanometer beam to the base line, the setting ($P_{5.0}$) was noted, and the flow was stopped. Similarly, deflections were recorded on dye-blood mixtures of 7.5 and 10 mg/liter at settings P_0 , $P_{2.5}$, and $P_{5.0}$. The calibration factors (K , mg/liter \cdot cm) are the reciprocals of the slopes of the straight lines drawn through the points obtained. In densitometer II (left panel) the increase in the calibration factor with increasing background dye level (2.5 and 5.0 mg/liter) amounts to a loss in instrumental sensitivity of about 1.5%/mg/liter

$$(\text{loss} = \frac{(1.01 - 0.94)/0.94}{5.0} = 1.5\%). \text{ In densitom-}$$

eter I, the sensitivity loss was 0.9%. The sensitivity loss in these densitometers varied from month to month but was usually about 1.1%/mg/liter of background dye (range = 0.7 to 1.5%).

The sensitivity of the densitometer was quite stable during each experiment. Standard dilutions of indocyanine green in blood were passed through the densitometer at the beginning and at the end of the experiment (6 or 7 hours later); in no case did readings differ by more than 3%.

During a few of the 2- to 3-minute periods of continuous sampling for the dye curves there

was a little drift in the output of the densitometers. This was most obvious during the recirculation and equilibration period following the inscription of the primary dye curve, when it was found occasionally that the equilibrium concentrations appeared to be different at the two sampling sites. Such curves were excluded from this study since, under such conditions, the shape of the curves could not be ascertained with accuracy.

RECORDING SYSTEMS

Two recording systems were used in parallel. The photokymographic assembly described by Wood¹⁸ was used to record: output of densitometer II (femoral artery), output of densitometer I (dorsalis pedis artery), respiration, aortic pressure, femoral artery pressure, femoral injection syringe travel, aortic injection syringe travel, superior vena cava pressure, electrocardiogram, binary marking-signal for coordinating this record with the analog tape record, and injection signal for superior vena caval injections. Selected data were recorded on 7-channel Ampex analog tape at three and three-fourths inches per second with carrier frequency of 3,400 cycles per second. These were: output of the densitometer at the femoral artery, output of the densitometer at the dorsalis pedis artery, aortic pressure, aortic injection syringe position, electrocardiogram, and audio and binary tape-marker signals used for search and synchronization during subsequent analog-to-digital conversion. The analog tape was used for analog computer analysis⁷ and, for the

purposes of this study, was converted into taped digital information by means of an analog-to-digital converter assembly described previously.¹⁴ Conversion rates for the dye curves and for the syringe travel were 139 and 23 samples per second, respectively.

Methods of Analysis

PREPARATION OF DATA

From the digital tape, the recorded dye curves were converted into concentration-time curves, with the midpoint of the injection (to the nearest 1/23 second) taken as the zero time. The slow sampling rate for the syringe travel was used in order to keep within the memory limits for the IBM 1620 digital computer used for the data reduction and analysis.

The dye calibration factors for each densitometer were calculated from the digitized tape record of the calibration dilutions. For each dye curve, the base line value was ascertained and subtracted from the total curve. The curves were smoothed by means of a 7- or 9-point moving average to reduce the artifact introduced by pulsatile flow, to which these densitometers are sensitive. The smoothed data were converted to terms of milligrams per liter and preserved on punched cards at 0.25-second intervals (each to the nearest 1/139 second). The punched cards were used as the data source throughout the remainder of the analysis. The appearance time, t_a , was chosen to be the time at which the concentration first equalled or exceeded 1.5% of the peak concentration, C_p .

GENERATION OF THE MODEL IN THE COMPUTER

The lagged normal density curve was generated from the differential equation by Simpson's method, expressed numerically at 0.25-second intervals, and truncated when its ordinate value decreased to less than 1.5% of the peak value.

CURVE-FITTING PROCEDURE

Fitting of the recorded curves with the model was accomplished on the computer by a method adapted from that of Hazelrig and co-workers.¹⁵ Programming was in Fortran II. The number of variable parameters for the trial adjustments could be reduced to two because the mean transit time of the recorded wave equals $\tau + t_c$ and the peak height of the model was adjusted to fit the peak of the dye curve.

The best σ and τ were obtained by a systematic search in the σ, τ plane. Trial parameters were initially assigned, and then the computer generated the curve having these parameters and also generated eight other curves having σ and τ values located at the corners and midpoints of the sides of a square surrounding the original trial point. The width of the square was set at 0.6 second or less. The pair of parameters forming a curve having the smallest coefficient of variation from the recorded curve was used as the center of the next trial square. The coefficients of variation for points previously tested were retained and not recalculated. When the center of the square was the best answer, the square size was reduced to 31% of the original width and the search was repeated until the central coordinates provided the best parameters

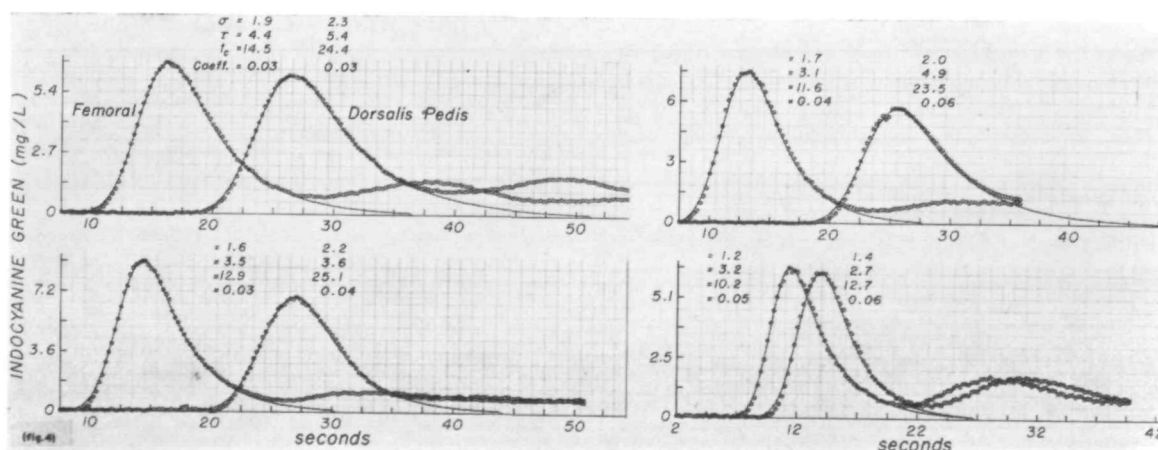


FIGURE 4

The lagged normal density curve fitted to curves recorded after injection of dye into the superior vena cava. Each panel shows the curves recorded (open circles) from the femoral artery and the dorsalis pedis artery of normal men. The parameters, σ , τ , and t_c of the model (solid line) fitting each curve, and the coefficient of variation of the fit are given above the curves.

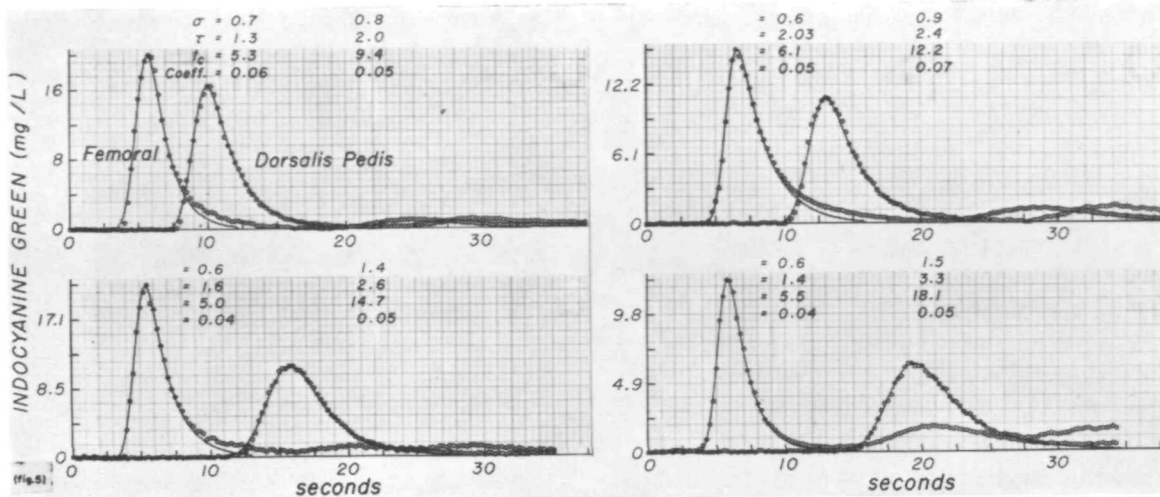


FIGURE 5

Lagged normal density curves fitted to curves recorded after injection of dye into the thoracic aorta.

and the square size was reduced again. When the center of this small square (9.6% of the original) was found to give the smallest coefficient of variation, the search was complete. Thus, σ and τ were obtained, at the worst, to the nearest 0.03 second.

The coefficient of variation, labelled "coeff" in figures 4, 5, and 6, is given by:

$$\left[\frac{\sum_{i=1}^n (F_i - C_i)^2}{n-1} \right]^{1/2} \cdot \frac{n}{\sum_{i=1}^n F_i} \quad (4)$$

in which F_i and C_i are the ordinate values at time, i , for the recorded and computed curves, respectively. The recorded and computed curves were plotted by the computer by means of an incremental x-y plotter.*

CALCULATION OF MOMENTS

Moments of the curve may be calculated from the recorded curve if the downslope is approximated in some fashion to exclude recirculation. The Hamilton extrapolation¹⁰ or some model, such as the lagged normal density curve, may be used (the difference is real, but slight). The first moment is the mean transit time:

$$\bar{t} = \frac{\int_0^{\infty} t \cdot C(t) dt}{\int_0^{\infty} C(t) dt} \quad (5)$$

The higher moments are calculated by using \bar{t} as the centroid:

$$\frac{1}{A} \int_0^{\infty} (t - \bar{t})^2 \cdot C(t) dt = \pi_2 = \text{variance} \quad (6)$$

The general equation for the n^{th} moment is:

$$\frac{1}{A} \int_0^{\infty} (t - \bar{t})^n \cdot C(t) dt = \pi_n = (\pi_2)^{n/2} \beta_{n-2} \quad (7)$$

in which A is the area, $\int_0^{\infty} C(t) dt$, of the

curve, and β_{n-2} is a family of parameters expressing the shape of the distribution curve (β_1 measures the skewness and β_2 , the flatness or kurtosis). For a normal density curve, β_1 is zero and β_2 is 3.0.

Results

Wide variation in the spread of recorded dilution curves was obtained by injecting at sites distant (superior vena cava) and close (aorta) to the sampling sites and by infusing ATP to produce large changes in flow in the leg and, secondarily, moderate changes in cardiac output. The result was that the curves used for analysis in this paper represented mean transit times from injection site to recording site ranging from 3 to 34 seconds. The difference between the mean transit times of paired femoral and dorsalis pedis curves is

*Calcomp model 565 made by California Computer Products, Downey, California.

the average time for the indicator to travel between these sites. On the basis that the volume of the arterial system in the leg is little affected by flow rate, the range of mean transit time differences, from 2.1 to 16.4 seconds, indicates that the fastest flow rate was eight times the slowest. When there was no ATP infusion, the average mean transit time difference was 10 to 12 seconds, while external iliac artery flow rates obtained at these times (by a method using constant-rate dye injection into the external iliac artery via the catheter numbered 4 under Methods) were 350 to 500 ml/min. The highest external iliac artery flow rates obtained during ATP infusion were greater than 3,000 ml/min.

MODEL FITTED TO RECORDED CURVES

One hundred eighteen dilution curves recorded from five subjects were fitted with the

lagged normal density curve. On each of the recorded curves, the appearance time, t_a ; the time constant of the downslope, T_D ; and the first and second moments, \bar{t} and π_2 , were calculated. The model was found to fit not only the broad dye curves produced by injection into the superior vena cava but also the sharply peaked curves produced by aortic injection. Because there were no significant differences, data from the five subjects were combined for consideration.

Figure 4 illustrates the relationship between representative curves recorded after injection of dye into the superior vena cava and the matching model. The average coefficient of variation for 60 curves was 0.043 (standard error of mean = 0.002).

Figure 5 shows the model fitted to curves recorded after dye injection into the aorta. The match was poorer in most instances (co-

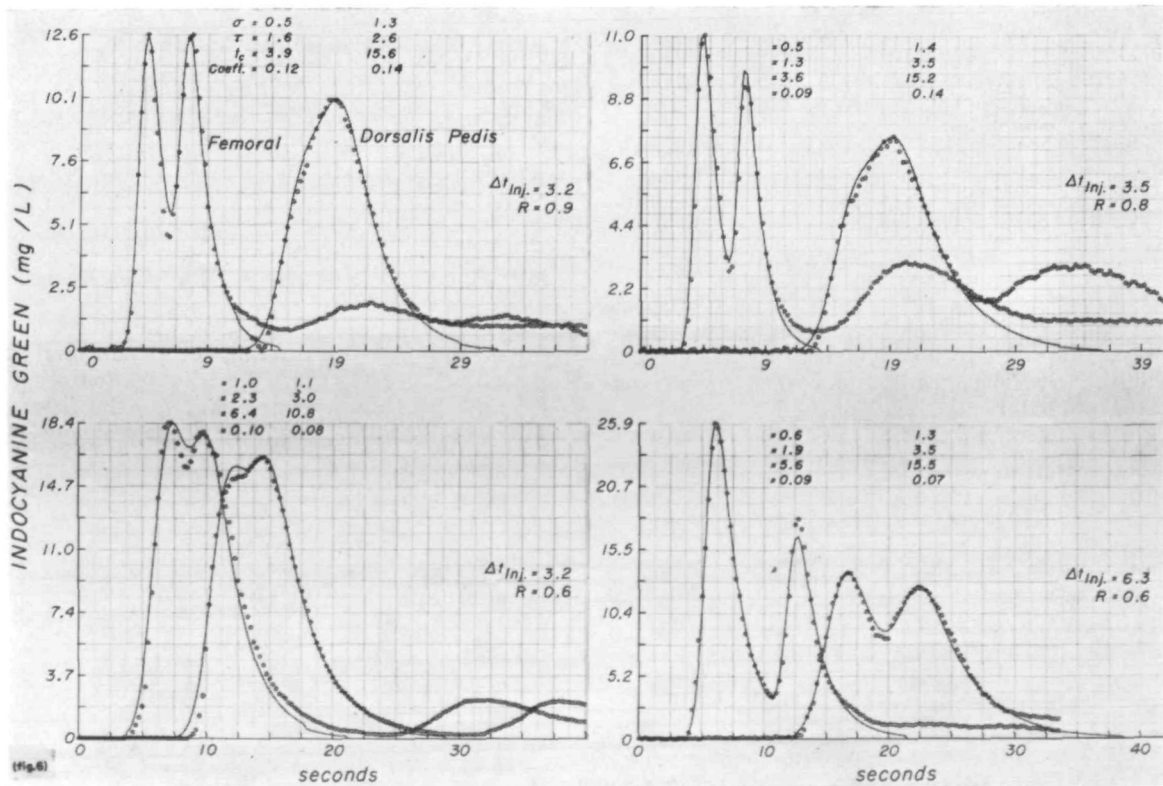


FIGURE 6

Curves recorded after two injections in the aorta, a few seconds apart (solid line), approximated by sum of two lagged normal density curves. ΔT_{inj} = time between the two injections. R = ratio of volume of second injection to volume of first injection.

efficients of variation averaged 0.069 ± 0.004), the model often departing from the recorded curve at the end of the downslope and particularly with the curves recorded from the femoral artery. These curves, which usually return to the base line before recirculation appears, are very short and are especially sensitive to the influences of dispersion at the injection site and of slurring by the sampling system.

When two slugs of dye are injected a few seconds apart into the thoracic aorta, the curve recorded at the femoral artery always reveals two distinct peaks while at the dorsalis pedis the two peaks may or may not be slurred together. The model is still applicable (fig. 6). To fit such a curve, the model is generated twice, the amplitude of the components being in proportion to the amount of dye in each injection, and with values of t_0 differing by the time between injections, the two similarly shaped components (having

the same σ and τ) are summed. The application of the model to these curves involves the same assumptions regarding constancy and stationarity of flow as does application to the simpler curves and, therefore, provides a more critical test of the model and of the stability of the physiologic state of the subject.

RELATIONSHIPS BETWEEN PARAMETERS OF THE MODEL AND THE MEAN TRANSIT TIME

The data indicate that the spread of the dye curves is linearly related to mean transit time (\bar{t}) and also that the shape of the curves is almost constant; if \bar{t} is known, σ and τ may be estimated approximately. Figure 7 shows σ and τ to be related linearly to \bar{t} . The right panel shows the relationship between σ and τ (average $\sigma/\tau = 0.44$), indicating the curve shape to be nearly constant. This and the fact that the square root of the variance, $(\sigma^2 + \tau^2)^{1/2}$ or $\pi_2^{1/2}$, was proportional to \bar{t} (fig. 8) provide the

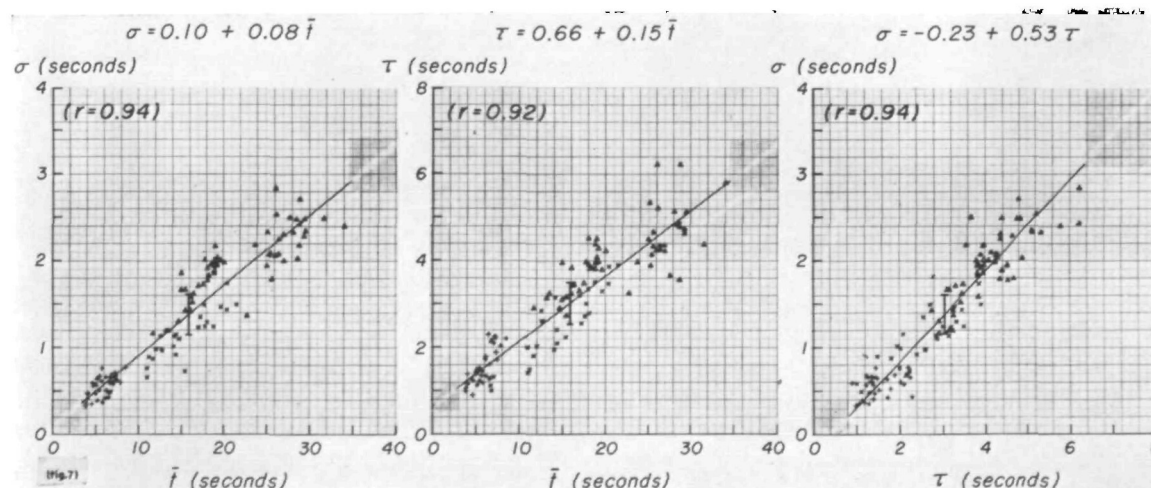


FIGURE 7

Parameters of the model simulating recorded dye curves. Left and center panels: the linear relationships (see table 1) between σ or τ and the mean transit time show that the temporal dispersion of indicator is inversely proportional to the average velocity of the blood between the injection and sampling sites. Right panel: the correlation of σ and τ indicates that the shape of the curves is fairly constant. In the left and middle panels the points for curves following SVC injection (open triangles for curves sampled at the femoral arteries, closed triangles for those from the dorsalis pedis arteries) are higher than those for aortic injections (plus signs for curves sampled at the femoral arteries, X's for those from the dorsalis pedis arteries) but the slopes of the regression equations (table 1) for the two groups are not significantly different. The positive intercepts indicate that dispersion in the central circulation is greater than in a peripheral artery. In these and subsequent graphs the length of the vertical line through the average point is two standard deviations. The correlation coefficient is r .

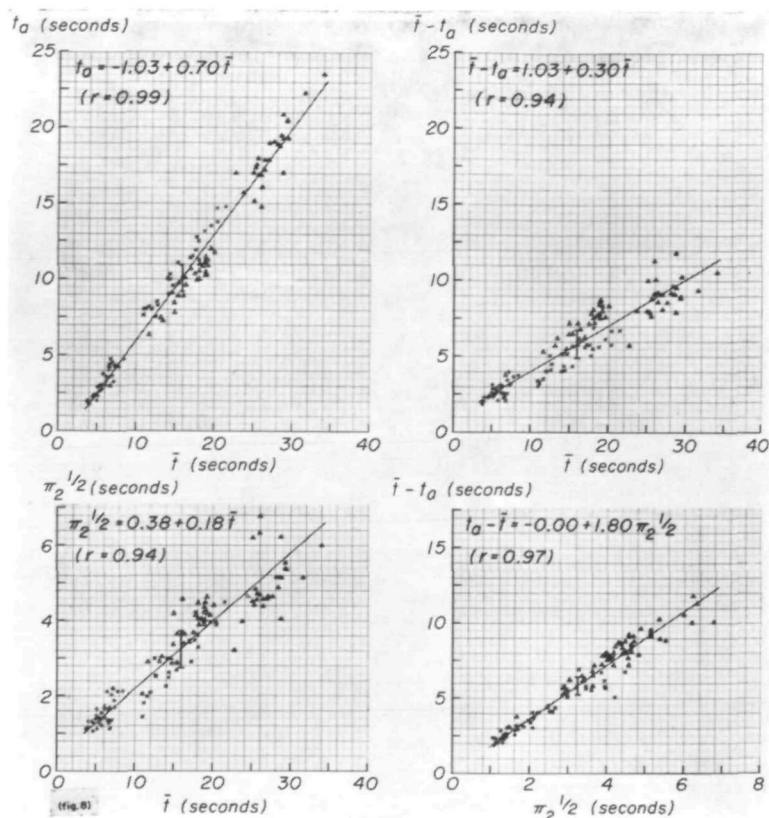


FIGURE 8

Nonparametric measures of the dispersion. t_a (left upper panel), $(\bar{t} - t_a)$ (right upper panel), and $\pi_2^{1/2}$ (square root of the variance) (left lower panel) are all linearly related to \bar{t} . The spread, $\bar{t} - t_a$, and $\pi_2^{1/2}$ are closely related to each other, as expected (right lower panel). These linear relationships indicate that temporal dispersion is related linearly to the time taken to travel a given distance and suggest that the spatial dispersion is unrelated to the flow rate through the limb. (Symbols as in fig. 7; for regression equations, see table 1.)

basis for the linear relationships of σ and τ with \bar{t} .

The regression lines for σ and τ with \bar{t} do not pass through the origin but have positive ordinate intercepts. The regression lines calculated for the data concerning each injection site (table 1) show σ and τ to be greater for curves recorded after injection into the superior vena cava than for those following aortic injection. The regression lines were approximately parallel but the intercepts differed. Since the magnitude of the intercepts is dependent on the dispersion occurring upstream from the femoral sampling site, and the magnitude of the slope is proportional to the dispersion occurring between the two sampling sites, two inferences may be drawn.

1. Since the intercepts are larger for curves recorded after injection into the superior vena cava than for those recorded after injection into the aorta, it follows that dispersion is proportionately greater during passage through the heart and lungs than through the aorta.
2. Since the slopes are not statistically different for the two injection sites, it may be concluded that either the injections cause no reactive error in the arterial system of the leg or whatever reactive error exists is the same for the two injection sites. These inferences cannot be based on the ratios σ/\bar{t} and τ/\bar{t} (table 2) but the fact that σ/\bar{t} and τ/\bar{t} are smaller for curves from the dorsalis pedis artery than for curves from the femoral artery does indicate that

TABLE 1

Regression Equations Relating Dispersion to Mean Transit Time

Injection into superior vena cava*			Injection into aorta†		
Equation	SD	r‡	Equation	SD	r‡
$\sigma = 0.44 + 0.0695\bar{t}$	0.23	0.84	$\sigma = 0.10 + 0.0703\bar{t}$	0.13	0.94
$\tau = 1.03 + 0.141\bar{t}$	0.51	0.78	$\tau = 0.48 + 0.151\bar{t}$	0.35	0.90
$\pi_2^{1/2} = 0.37 + 0.185\bar{t}$	0.65	0.82	$\pi_2^{1/2} = 0.36 + 0.177\bar{t}$	0.32	0.94
$(\bar{t} - t_a) = 1.77 + 0.290\bar{t}$	0.98	0.83	$(\bar{t} - t_a) = 1.04 + 0.263\bar{t}$	0.48	0.94
$t_a = -3.26 + 0.777\bar{t}$	0.98	0.98	$t_a = -1.25 + 0.759\bar{t}$	0.48	0.99

*Except for τ , equations are based on 60 points.

†Equations are based on 58 points.

‡r is the coefficient of correlation.

peripheral arterial dispersion is less than the sum of dispersion at the injection site and dispersion in the central circulation.

RELATIONSHIPS BETWEEN NONPARAMETRIC MEASURES OF THE SPREAD AND MEAN TRANSIT TIME

Further evidence for the linear increase of spread with \bar{t} is given in figure 8. The appearance time, t_a , and the appearance time - mean transit time difference, $\bar{t} - t_a$, are different ways of expressing the same simple measures of the spread. Their linear relationship with \bar{t} is in part dependent on the approximate constancy of shape of the curves. The variance, π_2 , is a calculation independent of shape. Its square root, $\pi_2^{1/2}$, is the standard deviation of the curve and is seen to be linearly related to \bar{t} . That the dispersion or spread is greater following injection into the superior vena cava than into the aorta is seen in the relationships of t_a , $\bar{t} - t_a$, and $\pi_2^{1/2}$ to \bar{t} in this figure and in table 1 where the regression lines for each injection site are given. The more negative the intercept in the plot of t_a against \bar{t} , the greater the dispersion of indicator in the circulation proximal to the femoral sampling site. The linear relationship between $\bar{t} - t_a$ and $\pi_2^{1/2}$ indicates again the constancy of shape of the curves.

RELATIONSHIPS BETWEEN MODEL PARAMETERS AND VALUES OBTAINED FROM THE RECORDED CURVES

Figure 9 provides more information on the close relationships between the parameters of the spread of the lagged normal density curve, σ and τ , and the spread of the recorded

curves as given by $\bar{t} - t_a$ and $\pi_2^{1/2}$. The linear relationships are expected from the data of figures 7 and 8. Because of the close correlations and the fact that σ and τ provide a complete description of the shape of the curve, it is apparent that σ and τ can be more useful in describing the data than $\bar{t} - t_a$ and $\pi_2^{1/2}$, which provide only a partial description.

Figure 10 relates parameters of the model to standard measurements made on the recorded curves. The model almost always had a slightly earlier appearance time and first portion of the upslope than did the recorded curve (figs. 4, 5, and 6). The ratios of theoretical to recorded appearance times averaged 0.94 ± 0.005 . T_D is the time constant of an exponential curve¹⁰ fitted to that portion of the downslope between 70 and 30% of the peak concentration, C_p ; the ratio of τ to T_D , was 0.98. Thus, σ had very little influence on the downslope in this region. The lagged normal density curve decreases to zero slightly faster than does the Hamilton extrapolation.

The relationship between the mean transit time of the model, $\tau + t_c$, and the calculated (see equation 5) mean transit time, \bar{t} , and the relationship between the square root of the variance of the model, $(\sigma^2 + \tau^2)^{1/2}$, and the square root of the variance, $\pi_2^{1/2}$ calculated (see equation 6) from the recorded curve would fall on the line of identity if the model fitted the curves exactly. However, the moments of the model are greater than the

TABLE 2
Ratios Between Parameters of Models Fitted to Recorded Curves and Mean Transit Time

Ratio	Injection into superior vena cava		Injection into aorta		All curves		Significance of difference (P)†
	Femoral artery N	Dorsalis pedis artery Mean ± SE	Femoral artery N	Dorsalis pedis artery Mean ± SE	N	Mean ± SE	
σ/\bar{t}	30	0.105 ± 0.001*	29	0.099 ± 0.004*	118	0.091 ± 0.001	< 0.01
τ/\bar{t}	30	0.228 ± 0.006*†	29	0.273 ± 0.007*†	118	0.213 ± 0.003	< 0.01
π_2/\bar{t}	30	0.233 ± 0.004*†	29	0.277 ± 0.007*†	118	0.223 ± 0.003	< 0.01
$(\bar{t} - t_n)/\bar{t}$	30	0.420 ± 0.006*†	29	0.455 ± 0.012*†	118	0.375 ± 0.004	< 0.01
t_n/\bar{t}	30	0.580 ± 0.006*†	29	0.545 ± 0.012*†	118	0.625 ± 0.004	< 0.01

* $P < 0.01$, difference between sampling sites.

† $P < 0.01$, difference between injection sites.

‡Based on all curves, i.e., for comparison of sampling sites, data from both injection sites were combined, and, for comparison of injection sites, data from both sampling sites were combined.

calculated moments because the Hamilton extrapolation is truncated at 1.5% C_p and, therefore, \bar{t} and π_2/\bar{t} are reduced significantly from the values obtained by extrapolation to zero concentration at infinite time.

Discussion

The experiments of Allen and Taylor¹⁷ on dispersion in water mains, of Taylor^{3,4} on dispersion in smooth and rough pipes, and of Hull and Kent² on dispersion in oil pipe lines indicate that it is appropriate to consider indicator dispersion in flowing fluids as a probability distribution of transit times. The most straightforward approach is to examine the dilution curve itself as Stephenson,¹⁸ Meier and Zierler,¹⁹ Korner,²⁰ and others have done. The information obtainable may be phrased in terms of the area, of the time of certain points of the curve (the appearance time, t_a , and the peak, t_p), and of the first few moments (mean transit time, variance, skewness, kurtosis). Fruitful attempts have been made to reduce the number of parameters to a minimum by the use of specific mathematical models which can be fitted to the recorded curve. The random walk,^{5,21,22} the log normal curve,²⁸⁻²⁶ a gamma variate equation,^{27,28} a triple exponential model,²⁹⁻³¹ a simple velocity probability model,³² and a variable path-length probability model³³ have been considered. Any such model may be criticized on the basis that it does not completely represent the physical situation, and, when the proponents of a model have extrapolated too far,²⁹⁻³¹ both theoretical objections^{34,35} and experimentally documented contradicting evidence^{36,37} have appeared.

Another approach has been to consider various laminar flow models.³⁸⁻⁴¹ Only the generalized approach of González-Fernández³⁸ and extensions of detailed and mathematically difficult approaches such as those of McDonald⁴² and Streeter et al.⁴³ seem appropriate to circulatory studies.

LAGGED NORMAL DENSITY CURVE AS A DESCRIPTION OF RECORDED DYE CURVES

The lagged normal density curve is a

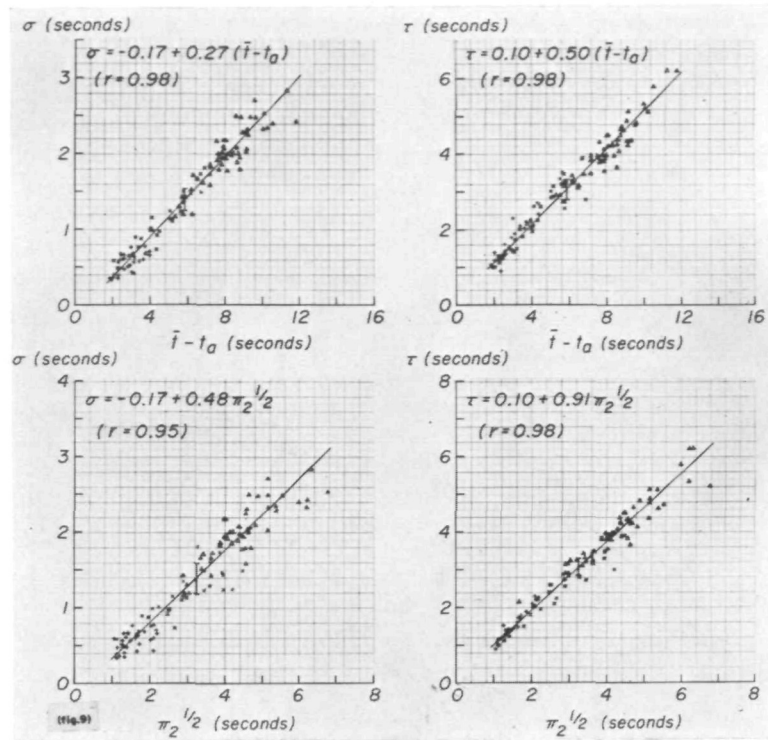


FIGURE 9

Interrelationships between parameters of model and characteristics of recorded dye curves estimating the dispersion.

probability model. It has the virtue of relative simplicity but is certainly not unique. Its particular virtue in this study is one common to any useful model: it provides a brief and fairly accurate description of recorded dye dilution curves of widely varying shape. In using it, high-frequency information concerning the details of the flow during each cardiac cycle is lost. The model is appropriate only when the cardiac cycle is short compared to (1) the mean transit time between the injection and sampling sites and (2) the passage time of the bolus of dye past a sampling site. These same limitations apply to the classical methods of estimating flow from a dye curve. The shape of the model is expressed completely by σ and τ ; the area, by its amplitude factor, m_i/Q ; the mean transit time, by $\tau + t_c$; and the variance, by $\sigma^2 + \tau^2$. Thus, it is probably easier to relate this model to terms with which most workers are already familiar than to so relate models such as the random walk,⁵ the log

normal curve,²³ or the mixing chamber model.²⁰

The choice of the model was based in part on physical analogy (which is not completely appropriate for blood flowing in the vascular system) and in part because this model describes transfer functions in the arterial system.⁷ But the lagged normal density curve does not represent a physical system; such representation would require a much more complex model. The dispersion defined by σ and τ defines intra-arterial plus catheter dispersion when the injection is made into the aorta; this might be defined more realistically by serial combinations of different random walk equations if flow were turbulent. However, the model also describes the distribution of transit times when the indicator passes through the pulmonary capillary bed. There is no apparent physiologic reason for there being any particular distribution of path lengths through the lung. The distribution could be multip peaked or skewed to the

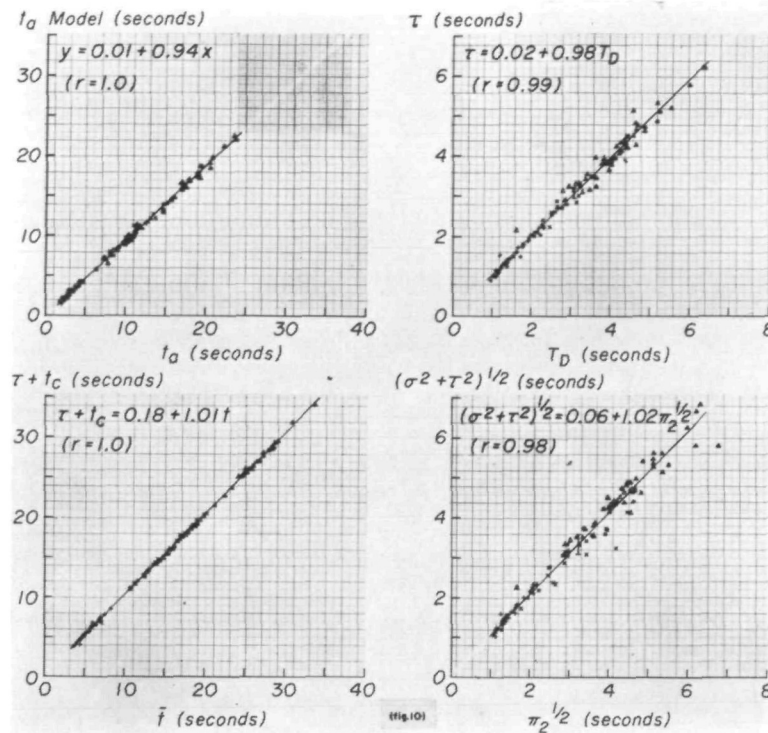


FIGURE 10

Relationships between recorded curves and the model. Left upper panel: the appearance time for the models fitted to the curves (t_a Model) were less than the recorded ones, t_a , indicating that the earliest recognized indicator had a lower velocity than the equation implied. Right upper panel: the values of τ were only slightly smaller than the time constants, T_D , showing that σ had little effect on the decay slope. Left lower panel: the mean transit times of the models, $\tau + t_c$, were 1% larger than the first moments, \bar{t} . Right lower panel: The square roots of the second moments of models, $(\sigma^2 + \tau^2)^{1/2}$, were almost 2% larger than those of the recorded curves, $\pi_2^{1/2}$.

left; a single-peaked distribution can be expected on an anatomic basis. But it must still be regarded primarily as coincidence that the distribution is almost the same through the heart and lungs as in the arterial system. The probable explanation is that the frequency distribution of pulmonary path lengths is more or less Gaussian, that the effect of ventricular chambers is somewhat like a first-order lag, and that the combined effect is a frequency distribution of transit times very similar to that produced in the arterial system. It should be clearly understood that τ defines no identifiable chamber volume and σ , no anatomic distribution of path lengths.

It is apparent from the ratios of t_a/\bar{t} and from the shapes of the curves that, in the

arteries, the velocity profile is very blunt compared to a parabola. It appears also that this flow profile and the rate of spatial dispersion of indicator did not vary significantly over the several-fold range of flows observed in the external iliac artery, because the relationships of the various parameters to \bar{t} were linear (table 1 and figs. 7 and 8). The lack of any transition from laminar to turbulent flow is in accord with McDonald's concept that blood flow is "disturbed flow," neither laminar nor turbulent.

The variation in curve shape obtainable with the lagged normal density curve can be obtained with the random walk and the log normal models only if considerable adjustments in time origin, time-scale factors, and randomizing factors are made. Because

of the necessity for such artifices the theoretical basis for these equations is invalidated, and they must be classed with the lagged normal density curve and the gamma variate as equations that merely describe the shape of the curve.

The excellence of the lagged normal density curve as a description of recorded curves is expressed not only by the coefficients of variation but also by the relationships shown in figure 10 (these are close to the line of identity). However, this also suggests that one should consider describing the dye curve in terms of its first few moments rather than by using a parametric model. This would be quite useful if moments higher than the third or fourth conveyed so little information that they could be ignored.

DISPERSION IN SPECIFIC SEGMENTS OF THE CIRCULATION

The data of figures 8 and 9 and of table 1 are concerned primarily with the dispersion between the two sampling sites. This is expressed in the slopes of the relationships, which are very similar to those for the transfer functions between the femoral and dorsalis pedis arteries.⁴⁴

Less precise, but still useful, information concerning the dispersion between the injection site and the femoral artery is given by the intercept values. The greater the intercept values for σ , τ , $\bar{t} - t_a$, or $\pi_2^{1/2}$ plotted against \bar{t} and the smaller the intercept for t_a versus \bar{t} , the greater the dispersion occurring in this segment (see figs. 8 and 9 and table 1). A similar type of information is given by the ratios to \bar{t} for curves sampled at the femoral artery (first and third columns of data in table 2). Both the intercept values and the ratios are functions of the dispersion due to three types of events: (1) dispersion at the injection site due to the energy of the injection and the disturbance in flow at the injection site, (2) dispersion within the sampling system, and (3) dispersion in the circulation.

A sudden injection of dye solution through an end- or side-holed catheter results in immediate dispersion of dye some distance

in all directions. The spread of this bolus is also dependent on the duration of injection because, during a 0.5-second injection, aortic blood may flow more than 10 cm. If the flow pattern is laminated and is undisturbed by the injection, dye movement will not likely represent blood movement. Even with a forceful injection which causes mixing, the labelling at the injection site is likely to be neither cross sectional nor flow tagging as defined by González-Fernández.³⁸ The labelling is probably not uniform (with respect to flow or volume) until there has been significant downstream movement of the bolus. The aortic injection probably produced more dispersion: the energy of injection was 1×10^6 g cm² sec⁻² and injection was at high velocity through a small catheter pointed upstream against the rapidly flowing aortic blood. The superior vena caval injection was at low velocity through a larger catheter pointed in a downstream direction in slowly flowing blood.

The dispersion due to the sampling system consists of a delay time plus a slurring of the concentration-time curve as it passes through the sampling apparatus. This may be characterized fairly well^{12, 45, 46} and a correction can be made for the distortion by a variety of methods.⁴⁶⁻⁴⁹ Certain of the curves recorded during these experiments have been corrected either by using a method similar to that of González-Fernández and co-workers⁴⁷ (by using the inverse of the convolution integral) or by using exponential lead circuits in an analog computer.⁷ The same model, the lagged normal density curve, has been found to fit the corrected curves even though they are more sharply peaked and less slurred out.⁷ Although the femoral sampling system was more complex, its dynamic response to a step input was only slightly slower than that for the dorsalis pedis sampling system (fig. 2). The difference between the mean transit times of the sampling systems was 0.25 second and was considered to be small enough to be ignored in the analysis.

The dispersion in the segment of the cir-

ulation between the sampling sites from which the paired curves are recorded is indicated by the slopes of the regression lines of table 1. The values of the slopes should not be affected by the dispersion at the injection site but would be influenced by any significant difference between the sampling systems.

The intercept values are probably little influenced by the sampling system, for the degree of dispersion in the tubing is similar to that produced by the vascular system, and the mean transit time of the sampling system is a significant proportion of \bar{t} of the recorded curves only for those recorded at the femoral artery after aortic injections. The appearance time:mean transit time ratios found by Cheesman⁴⁹ for catheter sampling systems were very similar to those usually observed in the human or the canine circulation and to those found in this study (table 2).

The ratios shown in table 2 may therefore be considered primarily as functions of dispersion at the injection site plus dispersion in the circulation between injection and sampling sites. The dispersion upstream to the femoral artery is always greater than that downstream to it because the ratios (σ/\bar{t} , τ/\bar{t} , $\pi_2^{1/2}/\bar{t}$ and $[\bar{t} - t_n]/\bar{t}$) are all less for curves recorded at the dorsalis pedis artery than for those recorded at the femoral artery.

The dispersion subsequent to superior vena caval injections is greater than that after aortic injections. The evidence is that the intercept values are higher (regression lines of table 1) for the former. The positive intercept for aortic injections indicates that dispersion at injection site plus dispersion in the aorta due to the turbulent flow, especially at the bifurcation,⁴² is greater than dispersion in the arteries of the leg.

In their figure 7, Edwards and Korner⁵⁰ plotted variance against mean transit time for curves recorded from the femoral artery of dogs after sudden injections of dye into either the inferior vena cava at the renal veins or into the pulmonary artery. Their data showed the ratio, $\pi_2^{1/2}/\bar{t}$, to be 0.2 to 0.3. In general their data indicate $\pi_2^{1/2}/\bar{t}$

to be greater and t_n/\bar{t} to be smaller for curves recorded after pulmonary artery injection than for curves recorded after inferior vena caval injection. This suggests that the dispersion occurring during the traversal of the inferior vena cava is less, relative to the mean transit time, than the dispersion occurring in the heart, lungs, and aorta. In other circumstances this may not be so, for the streamlining of flow that occurs in the inferior vena cava produces a wide range of transit times through the segment. For example, radiopaque indicators have been observed to take nearly a minute to be washed out of the inferior vena cava below the diaphragm in anesthetized dogs.

Korner,²⁰ in his table 5, gave the regression equation:

$$\log \pi_2 (\text{sec}^2) = 3.699 - 2.432 \log \text{flow (ml/min)} + 2.020 \log \text{volume (ml)} \quad (12)$$

for 55 dye curves recorded from the femoral artery of dogs after injection of dye into either the pulmonary artery, right ventricle, or superior vena cava. Since $\bar{t} = \text{volume}/\text{flow}$, this equation can be rewritten:

$$\log \pi_2 = 3.699 - 0.412 \log \text{flow} + 2.020 \log \bar{t} \quad (13)$$

in which \bar{t} is in units of minutes. At an average value for flow of 2,000 ml/min, the relationship reduces to $\pi_2^{1/2} = 0.26 \bar{t}(\text{sec})$ which is quite comparable to the ratio, $\pi_2^{1/2}/\bar{t} = 0.233$, shown in table 2 of this paper for curves recorded at the femoral artery after superior vena caval injection.

The most effective mechanism for circulatory dispersion occurs with the great diversity of path lengths and flow rates through the capillary and venous beds of the peripheral organs and tissues. It is clear from this study that there is no great difference in the dispersion of a bolus of material in the central circulation or peripheral arteries. The ratio of dispersion to transit time was largest following superior vena caval injection probably because of the diversity of path lengths and flows in the various segments of the lung and because of the mixing-chamber effects of the left atrium and left ventricle. The

reason that dispersion in the aorta is greater than in the peripheral artery is not that it is more turbulent (for this would probably mean less dispersion) but that there is greater longitudinal mixing due both to the greater pulsation of flow and to eddy formation at major branches.

ASYMMETRY OF THE CONCENTRATION-TIME CURVE

If the spatial distribution of indicator particles in the bloodstream were symmetric, concentration-time curves recorded at any site must be skewed to the right (the tail prolonged) if the indicator is being dispersed during its transit.

Taylor^{3, 4} and Hull and Kent² observed that indicator concentration-time curves become more symmetric as the indicator dispersed in proportion to the square root of the distance travelled. One would expect this from the central limit theorem. This theorem states that, for systems which are predominantly linear, as the number of events increases the distribution tends toward normality. Therefore, with an increase in \bar{t} , the theorem would predict a decrease in skew, kurtosis, and the ratio of τ to σ . The last relationship is $\tau/\sigma = 3.8 - 0.093 \bar{t}$ ($SD = 5.1$; $r = 0.47$). Similar evidence is seen in figure 7 (right panel) and in the relationships of σ and τ to $\pi_2^{1/2}$ (fig. 9). These data indicate the tendency for τ to form a smaller portion of the spread of the broader curves. Korner²⁰ observed that the asymmetry of curves recorded at the femoral artery of dogs decreased as the injection site was changed from pulmonary artery to right ventricle to superior vena cava, i.e., as the distance travelled was increased.

Dow⁵¹ found the greatest asymmetry in curves recorded at the femoral artery after left ventricular injection. The reason for this may be that not only is the path length short but ventricular mixing is poor and dye may be sequestered to some extent in the apex. With complete ventricular mixing, the concentration-time curve in the ventricle would be a single exponential in step form which is highly skewed and leptokurtotic. It is probable that the ascending aortic arch has a similar effect since there is no forward

flow there during diastole. Edwards and Korner⁵⁰ observed a similar phenomenon. Curves recorded at the femoral artery were more asymmetric after right atrial injection than after caval injection. They interpreted this as due to nonuniformity of clearance from blood near the wall of the atrium.

Summary

1. Indicator dilution curves (concentration versus time) were recorded from the femoral and dorsalis pedis arteries of normal men after injections of indocyanine green into the superior vena cava or thoracic aorta. A four-parameter mathematical model, the lagged normal density curve, adequately described the form of the portion of these curves representing indicator passing by the sampling site for the first time.

2. The curves were observed to be of constant shape, the spread of the curve being approximately linearly related to the mean transit time \bar{t} . The spread was dependent on the injection site; dispersion was shown to be greatest in the central circulation, less in the aorta, and still less in the arteries of the leg. For the latter segment, the mean transit time \bar{t} . The spread was dependent $0.3 \bar{t}$, the square root of the variance was $0.18 \bar{t}$, and the parameters of the lagged normal density curve, σ and τ , were $0.09 \bar{t}$ and $0.16 \bar{t}$, respectively.

3. The linear relationships between parameters of the recorded curves and the mean transit times indicate that the effect of rate of flow, over a range from resting values to four to six times above resting values, has almost no influence on the dispersion. This suggests that the flow characteristics are essentially unchanged over this range. Such linear relationships always occur with laminar flow but cannot prove its existence because turbulent flow can also produce this result. The similarity of the linear relationships at low flow rates to those at high flow rates, where turbulence almost certainly is present, suggests that arterial flow is usually turbulent. Turbulence may be expected at relatively low flow rates in nonhomogeneous fluids

driven by a pulsatile head of pressure through elastic, branched, tapering, curved tubes.

Acknowledgment

The help of Dr. Homer Warner, Department of Biophysics and Bio-engineering, Latter-Day Saints Hospital, University of Utah, Salt Lake City, was essential in the analog computer programming which led to the choosing of the circulatory model. The authors express their appreciation to their colleagues who were subjects and to those who were a part of the experimental team, Dr. H. W. Marshall, W. F. Sutterer, Lucille Cronin, Donald Hegland, Julius Zarins, and Irene Donovan. The personnel of the Mayo Clinic computer facility helped in carrying out the voluminous data analysis, and Mrs. Jean Frank and her co-workers prepared the illustrations.

References

1. GRIFFITHS, A.: On the movement of a coloured index along a capillary tube, and its application to the measurement of the circulation of water in a closed circuit. *Proc. Phys. Soc., London* 23: 190, 1911.
2. HULL, D. E., AND KENT, J. W.: Radioactive tracers to mark interfaces and measure intermixing in pipelines. *Ind. Eng. Chem.* 44: 2745, 1952.
3. TAYLOR, G.: Dispersion of soluble matter in solvent flowing slowly through a tube. *Proc. Roy. Soc., London* 219A: 186, 1953.
4. TAYLOR, G.: The dispersion of matter in turbulent flow through a pipe. *Proc. Roy. Soc., London* 223A: 446, 1954.
5. SHEPPARD, C. W.: Mathematical considerations of indicator dilution techniques. *Minn. Med.* 37: 93, 1954.
6. BASSINGTHWAIGHTE, J. B., WARNER, H. R., AND WOOD, E. H.: A mathematical description of the dispersion of indicator in blood traversing an artery. (abstr.) *Physiologist* 4: 8, 1961.
7. BASSINGTHWAIGHTE, J. B., WARNER, H. R., AND WOOD, E. H.: Analog computer analysis of dispersion of indicator in the circulation. *Am. J. Med. Electron.* In press.
8. WOOD, E. H.: Definitions and symbols for terms commonly used in relation to indicator-dilution curves. *Circulation Res.* 10: 379, 1962.
9. FELLER, W.: *An Introduction to Probability Theory and Its Applications.* vol. 1. New York, John Wiley and Sons, Inc., 1950.
10. FOX, I. J., AND WOOD, E. H.: Indocyanine green: physical and physiological properties. *Proc. Staff Meet. Mayo Clin.* 35: 732, 1960.
11. GRACE, J. B., FOX, I. J., CROWLEY, W. P., JR., AND WOOD, E. H.: Thoracic-aorta flow in man. *J. Appl. Physiol.* 11: 405, 1957.
12. FOX, I. J., SUTTERER, W. F., AND WOOD, E. H.: Dynamic response characteristics of systems for continuous recording of concentration changes in a flowing liquid (for example, indicator-dilution curves). *J. Appl. Physiol.* 11: 390, 1957.
13. WOOD, E. H.: Special instrumentation problems encountered in physiological research concerning the heart and circulation in man. *Science* 112: 707, 1950.
14. WOOD, E. H., SUTTERER, W. F., MARSHALL, H. W., AND NOLAN, A. C.: Use of the human centrifuge to study circulatory, respiratory and neurologic physiology in normal human beings and a description of an electronic data processing system designed to facilitate these studies. Aerospace Medical Division, Wright-Patterson Air Force Base, Tech. Doc. Rep. 63-105 (Dec.) 1963.
15. HAZELRIG, J. B., ACKERMAN, E., AND ROSEVEAR, J. W.: An iterative technique for conforming mathematical models to biomedical data. *Proc. 16th Ann. Conf. Eng. Med. Biol.* 5: 8, 1963.
16. KINSMAN, J. M., MOORE, J. W., AND HAMILTON, W. F.: Studies on the circulation. I. Injection method: Physical and mathematical considerations. *Am. J. Physiol.* 89: 322, 1929.
17. ALLEN, C. M., AND TAYLOR, E. A.: The salt velocity method of water measurement. *Mech. Eng.* 46: 13; 51, 1924.
18. STEPHENSON, J. L.: Theory of the measurement of blood flow by the dilution of an indicator. *Bull. Math. Biophys.* 10: 117, 1948.
19. MEIER, P., AND ZIERLER, K. L.: On the theory of the indicator-dilution method for measurement of blood flow and volume. *J. Appl. Physiol.* 6: 731, 1954.
20. KORNER, P. I.: Some factors influencing the dispersion of indicator substances in the mammalian circulation. *In Progress in Biophysics and Biophysical Chemistry.* J. A. V. Butler, B. Katz, and R. E. Zirkle, vol. 11. New York, Pergamon Press, 1961, pp. 111-176.
21. SHEPPARD, C. W., JONES, M. P., AND COUCH, B. C.: Effect of catheter sampling on the shape of indicator-dilution curves: Mean concentration versus mean flux of outflowing dye. *Circulation Res.* 7: 895, 1959.
22. SHEPPARD, C. W., JONES, M. P., AND MURPHREE, E. L.: Shapes of indicator-dilution curves obtained from physical and physiological labyrinths. *Circulation Res.* 9: 936, 1961.
23. STOW, R. W., AND HETZEL, P. S.: An empirical formula for indicator-dilution curves as obtained in human beings. *J. Appl. Physiol.* 7: 161, 1954.
24. CHINARD, F. P., TAYLOR, W. R., NOLAN, M. F., AND ENNS, T.: Renal handling of glucose in

- dogs. *Am. J. Physiol.* 196: 535, 1959.
25. CHINARD, F. P., ENNS, T., AND NOLAN, M. F.: Contributions of bicarbonate ion and of dissolved CO₂ to expired CO₂ in dogs. *Am. J. Physiol.* 198: 78, 1960.
 26. CHINARD, F. P., ENNS, T. AND NOLAN, M. F.: Indicator-dilution studies with "diffusible" indicators. *Circulation Res.* 10: 473, 1962.
 27. EVANS, R. L.: Two comments on the estimation of blood flow and central volume from dye-dilution curves. *J. Appl. Physiol.* 14: 457, 1959.
 28. THOMPSON, H. K., JR., STARMER, C. F., WHALEN, R. E., AND MCINTOSH, H. D.: Indicator transit time considered as a gamma variate. *Circulation Res.* 14: 502, 1964.
 29. NEWMAN, E. V., MERRELL, M., GENECIN, A., MONGE, C., MILNOR, W. R., AND MCKEEVER, W. P.: The dye dilution method for describing the central circulation: An analysis of factors shaping the time-concentration curves. *Circulation* 4: 735, 1951.
 30. NYLIN, G., AND CELANDER, H.: Determination of blood volume in the heart and lungs and the cardiac output through the injection of radiophosphorus. *Circulation* 1: 76, 1950.
 31. LEWIS, A. E.: Estimation of plasma volume of the heart. *Am. J. Physiol.* 172: 203, 1953.
 32. GIDDINGS, J. C., AND EYRING, H.: A molecular dynamic theory of chromatography. *J. Phys. Chem.* 59: 416, 1955.
 33. TURNER, G. A.: The flow structure in packed beds: A theoretical investigation utilizing frequency response. *Chem. Eng. Sci.* 7: 156, 1958.
 34. ZIERLER, K. L.: Theoretical basis of indicator-dilution methods for measuring flow and volume. *Circulation Res.* 10: 393, 1962.
 35. GRODINS, F. S.: Basic concepts in the determination of vascular volumes by the indicator-dilution methods. *Circulation Res.* 10: 429, 1962.
 36. MARSHALL, R. J., WANG, Y., AND SHEPHERD, J. T.: Components of the "central" blood volume in the dog. *Circulation Res.* 8: 93, 1960.
 37. MARSHALL, R. J., AND SHEPHERD, J. T.: Interpretation of changes in "central" blood volume and slope volume during exercise in man. *J. Clin. Invest.* 40: 375, 1961.
 38. GONZÁLEZ-FERNÁNDEZ, J. M.: Theory of the measurement of the dispersion of an indicator in indicator-dilution studies. *Circulation Res.* 10: 409, 1962.
 39. ROSSI, H. H., POWERS, S. H., AND DWORK, B.: Measurement of flow in straight tubes by means of the dilution technique. *Am. J. Physiol.* 173: 103, 1953.
 40. COULTER, N. A., JR., AND PAPPENHEIMER, J. R.: Development of turbulence in flowing blood. *Am. J. Physiol.* 159: 401, 1949.
 41. SHERMAN, H., SCHLANT, R. C., KRAUS, W. L., AND MOORE, C. B.: A figure of merit for catheter sampling systems. *Circulation Res.* 7: 303, 1959.
 42. McDONALD, D. A.: *Blood Flow in Arteries.* Baltimore, Williams and Wilkins Company, 1960, p. 328.
 43. STREETER, V. L., KEITZER, W. F., AND BOHR, D. F.: Pulsatile pressure and flow through distensible vessels. *Circulation Res.* 13: 3, 1963.
 44. BASSINGTHWAICHTE, J. B., WOOD, E. H., AND WARNER, H. R.: Distribution of the traversal times of blood flowing through an artery. (abstr.) *Physiologist* 6: 135, 1963.
 45. LACY, W. W., EMMANUEL, R. W., AND NEWMAN, E. V.: Effect of the sampling system on the shape of indicator dilution curves. *Circulation Res.* 5: 568, 1957.
 46. COOPER, J. K., SCHWEIKERT, J. R., ARNOLD, T. G., JR., AND LACY, W. W.: Removal of distortion from indicator dilution curves with analog computer. *Circulation Res.* 12: 131, 1963.
 47. GONZÁLEZ-FERNÁNDEZ, J. M., CHEESMAN, R. J., AND WOOD, E. H.: Mathematical analysis for the recovery of a dye-dilution curve distorted by the sampling-recording system. (abstr.) *Physiologist* 2: 46, 1959.
 48. PARRISH, D., GIBBONS, G. E., AND BELL, J. W.: A method for reducing the distortion produced by catheter sampling systems. *J. Appl. Physiol.* 17: 369, 1962.
 49. CHEESMAN, R. J.: Distortion of indicator-dilution curves by the sampling-recording system and a suggested method for its correction. Thesis, Graduate School, University of Minnesota, 1961.
 50. EDWARDS, A. W. T., AND KORNER, P. I.: Factors determining the dispersion of dye in indicator dilution curves in the normal mammalian circulation. *Clin. Sci.* 17: 265, 1958.
 51. Dow, P.: Dimensional relationships in dye-dilution curves from humans and dogs with an empirical formula for certain troublesome curves. *J. Appl. Physiol.* 7: 399, 1954.